

Long-Term Monitoring and Interpretation of Flares in the H₂O Maser Emission of IRAS 16293–2422

P. Colom¹, E. E. Lekht^{2*}, M. I. Pashchenko², G. M. Rudnitskii², and A. M. Tolmachev³

¹*LESIA, Observatoire de Paris–Meudon, CNRS, UPMC, Université Paris–Diderot,
5 place Jules Janssen, 92195 Meudon Cedex, France*

²*Sternberg Astronomical Institute, Lomonosov Moscow State University,
Universitetskii pr. 13, Moscow, 119991 Russia*

³*Pushchino Radio Astronomy Observatory, Astro Space Center, Lebedev Physical Institute,
Russian Academy of Sciences, Pushchino (Moscow region), Russia*

Received August 12, 2015; in final form, December 25, 2015

Abstract—The results of a study of the H₂O and OH maser emission from the cool IR source IRAS 16293–2422 are presented. The observations analyzed were obtained in H₂O lines with the 22-m telescope of the Pushchino Radio Astronomy Observatory during 1999–2015 and in OH lines with the Nançay radio telescope (France). A large number of very strong flares of the H₂O maser were detected, reaching fluxes of tens of thousands of Jansky. Individual features can form organized structures resembling chains ~ 2 AU in length with a radial-velocity gradient along them. The observed drift of the H₂O emission (2003–2004) in space and velocity (from 4.3 to 5.3 km/s) is not due solely to proper motion of the features. The other origin of the drift is a drift of the emission maximum during a flare as the shock consecutively excites spatially separated features in the structure in the form of a chain. The OH-line observations at 18 cm show that the emission remains unpolarized and thermal, with a line width of 0.7 km/s, which corresponds to a cloud temperature of ~ 30 K.

DOI: 10.1134/S1063772916080059

1. INTRODUCTION

The low-mass protoplanetary system IRAS 16293–2422 is a good representative of the class of cool IR sources. It is situated in the ρ Oph dark cloud, probably at a distance of 120 pc from the Earth [1]. The object is a source of far-IR emission. It was not detected at $25 \mu\text{m}$; its spectral energy distribution (SED) from $25 \mu\text{m}$ and 2.7 mm is in good agreement with the SED for a blackbody with a temperature of about 40 K. The bolometric luminosity of IRAS 16293–2422 is estimated to be $36 L_{\odot}$ [2].

Interferometric observations of the IR source at $2.7 \mu\text{m}$ have shown that it has a disk structure 1800 AU by 800 AU in size [3]. Gas and dust with a mass of $1\text{--}6 M_{\odot}$ rotate about the minor axis. IRAS 16293–2422 is a binary system, whose components A and B are separated by $5''$ (800 AU) and are embedded in a high-density molecular core (e.g., [4, 5]). Dusty submillimeter sources with an angular separation of $0.6''$ were detected in component A [6]. Component B is probably strongly fragmented.

The ρ Oph dark cloud has been repeatedly observed in CO molecular lines (e.g., [7, 8]). The observations of Wilking and Lada [9] in the C¹⁸O line show that the size of the cloud's central part (its core) is 1×2 pc. The cloud contains large-scale ($\sim 1'$) bipolar molecular outflows, observed in CO, and a magnetic field that is perpendicular to the major axis of the disk [10, 11]. One of the outflows is associated with source A; its velocity is 4 km/s. The other outflow has not been found to be associated with any object. The source A is also associated with a compact SiO molecular outflow [12].

The mass of the central protostar is estimated to be $\sim 0.3 M_{\odot}$ (e.g., [13]), and the dynamical mass of the molecular core to be about $2.3 M_{\odot}$. The matter density in the molecular core exceeds 10^8 cm^{-3} . All this indicates that IRAS 16293–2422 is at a very early stage in the formation of the central star.

A fairly large number of observations in the 1.35-cm H₂O line have been obtained toward IRAS 16293–2422. Wilking and Claussen [14] detected H₂O maser emission. Terebey et al. [15] demonstrated that the H₂O maser emission comes from a region $0.6''$ (~ 96 AU) in size, and is related

*E-mail: lekht@sai.msu.ru

only to source A. Chandler et al. [16] found that two submillimeter sources, Aa and Ab, were situated at the position of component A. According to [17], the H₂O maser emission is located near the submillimeter source Aa.

Monitoring by Furuya et al. [18] revealed rapid variations on a time scale of several days. Imai et al. [19] plotted maser-emission maps for three epochs in 1991 and 1994, and detected proper motions of three maser features [20]. Very strong features with short lifetimes appeared at velocities with blue and red shifts relative to the velocity of the CO molecular cloud (4 km/s).

Emission (unpolarized) in the OH 1665 and 1667 MHz main lines was also observed in the direction of IRAS 16293–2422, which, according to [21], is thermal. No methanol maser emission has been detected. The absence of hydroxyl and methanol maser or continuum emission is typical of very young objects.

2. OBSERVATIONS AND DATA USED

IRAS 16293–2422 (RA(2000) = 16^h32^m22.8^s, Dec(2000) = –24°28′35.8″) was included in a program of monitoring in the 1.35-cm water-vapor line using the 22-m Pushchino radio telescope in 1999. The signal was processed using a filter-type spectrum analyzer with a radial-velocity resolution of 0.101 km/s. Since late 2005, we have used a 2048-channel autocorrelation-type analyzer with a resolution of 0.0822 km/s. For a point source, an antenna temperature of 1 K corresponds to a flux density of 25 Jy. All our spectra have been corrected for absorption in the Earth’s atmosphere; this is important, as the source’s altitude above the horizon was only 10° – 11°.

We also obtained several series of observations of IRAS 16293–2422 in the 18-cm hydroxyl lines using the radio telescope of the Meudon Observatory’s Nançay Radio Astronomy Station (France) at various epochs, beginning in 2007.

Figures 1–6 present the H₂O maser emission spectra observed between 1999 and 2015. Since the flux range is large, the figures are shown using different vertical scales. Emission features that cross features in earlier spectra are plotted using dotted curves. The observation epochs in dd.mm.yyyy format are indicated for each spectrum. The horizontal axes plot the radial velocities relative to the Local Standard of Rest. The two-sided vertical arrows indicate the flux scale in Jansky. During strong flares, we observed with time intervals from one to several days. These spectra are not plotted, but we used them when analyzing the evolution of the flares. No signal was detected in the spectra between April and September 2014. An averaged spectrum for this time

interval is presented in Fig. 6. However, this average spectrum does not display any signal in excess of 5 Jy.

Figure 7 displays the radial-velocity variations of the main H₂O emission features. Features observed during epochs of high activity (strong flares in excess of 700 Jy) are plotted as open circles. The epochs of minimum activity are marked by vertical line segments in the lower part of the figure. The horizontal dash–dot line marks the velocity of the CO molecular cloud (4 km/s). There were no observations during the time interval between the two vertical dashed lines (from mid-2006 to the end of 2007) for technical reasons.

It is striking that the positions of most features in Fig. 7 are not chaotic, and tend to group along certain directions, indicating regular behavior in their evolution. We approximated the positions of maximum flux for features with similar radial velocities using the numbered straight dashed lines. We used two criteria for this identification: that the scatter of the data points not exceed the thermal line width, and that the flux exceed 700 Jy at at least one epoch (i.e., we are dealing with a sufficiently strong flare). The dashed lines may reflect a drift of the maximum emission from such structures in radial velocity.

Configurations 5 and 6 in Fig. 7 have a complex structure. Their individual elements are plotted using fragments of solid lines. The structure of configuration 5 is unordered in velocity, and consists of four individual elements. Configuration 6 displays a tendency for emission to move towards lower velocities (dashed line).

We observed in the main 18-cm hydroxyl lines in 2007, 2013, 2014, and 2015, in both linear and circular polarization. Observations in the satellite 1612 and 1720 MHz lines were obtained in 2014 and 2013–2014, respectively. We detected no emission in the 1612 MHz line. The results of these observations are presented in Fig. 8. We show spectra for the main lines averaged over the time of our observations, 2007–2015. Profiles are shown for the total emission (the sum of the emission in right- and left-circular polarizations, which are equal for unpolarized radiation).

3. DISCUSSION

We did not find periodic variations of the H₂O maser emission of the sort we observed earlier for many cool IR sources. We can speak only of the presence of some cyclic character of the activity of the H₂O maser. Our best estimate of the duration of the activity cycles is based on the emission minima. This analysis suggests that the duration of the activity cycles varied considerably in the range from 0.9 to 3.4 yrs. The activity cycles also differed from each

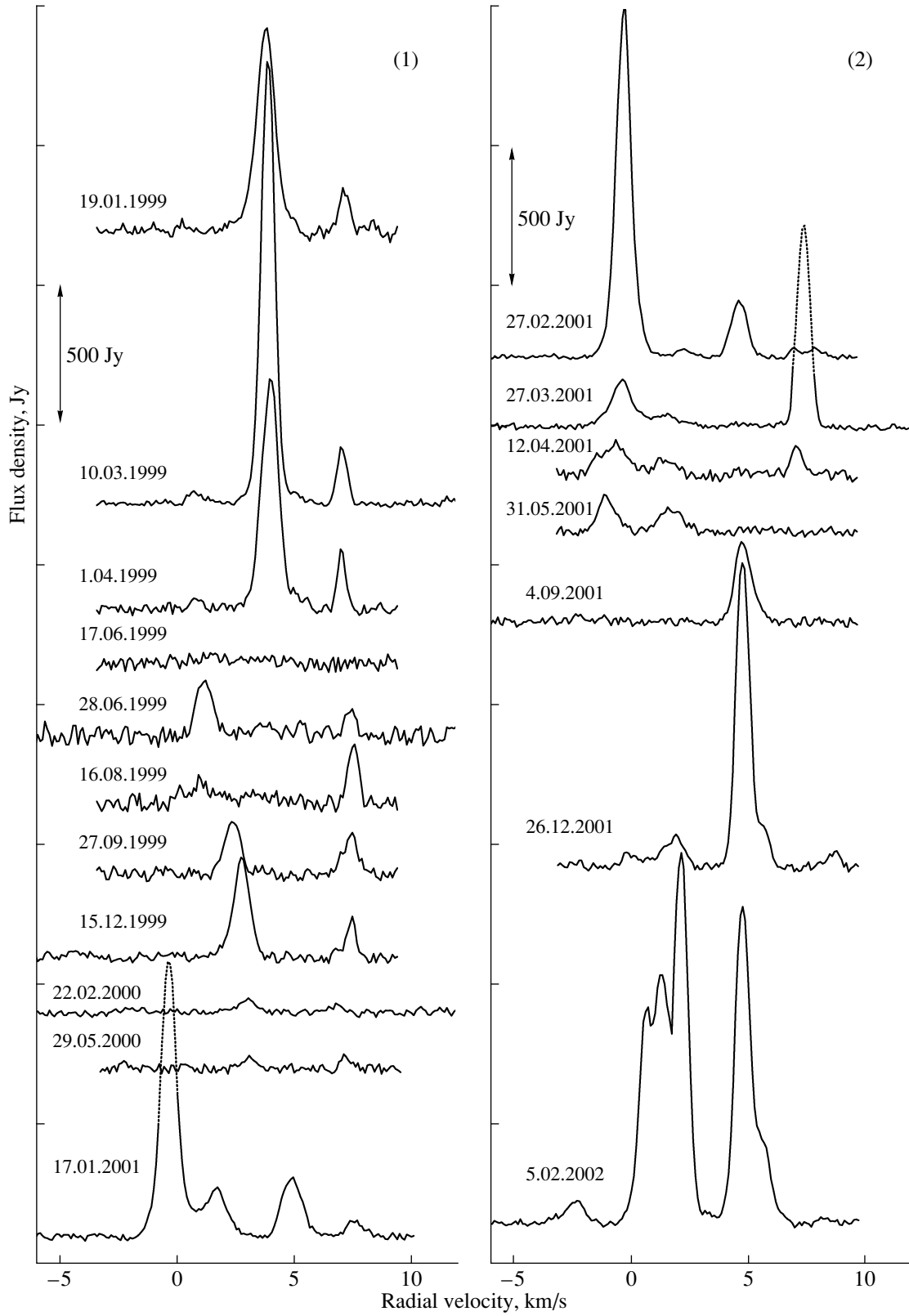


Fig. 1. H₂O maser spectra for IRAS 16293-2422 in 1999-2002.

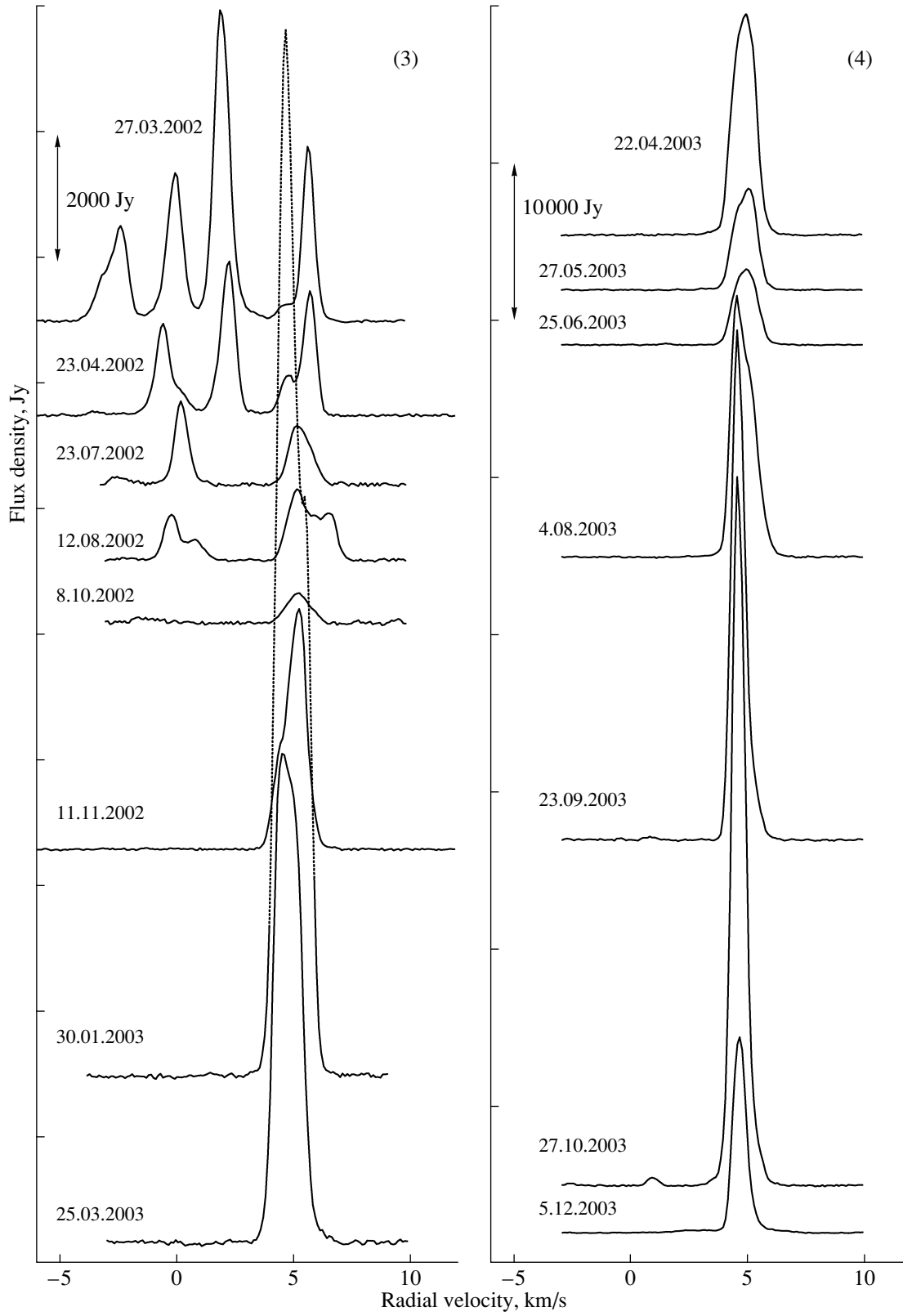


Fig. 2. H₂O maser spectra for IRAS 16293–2422 in 2002–2003.

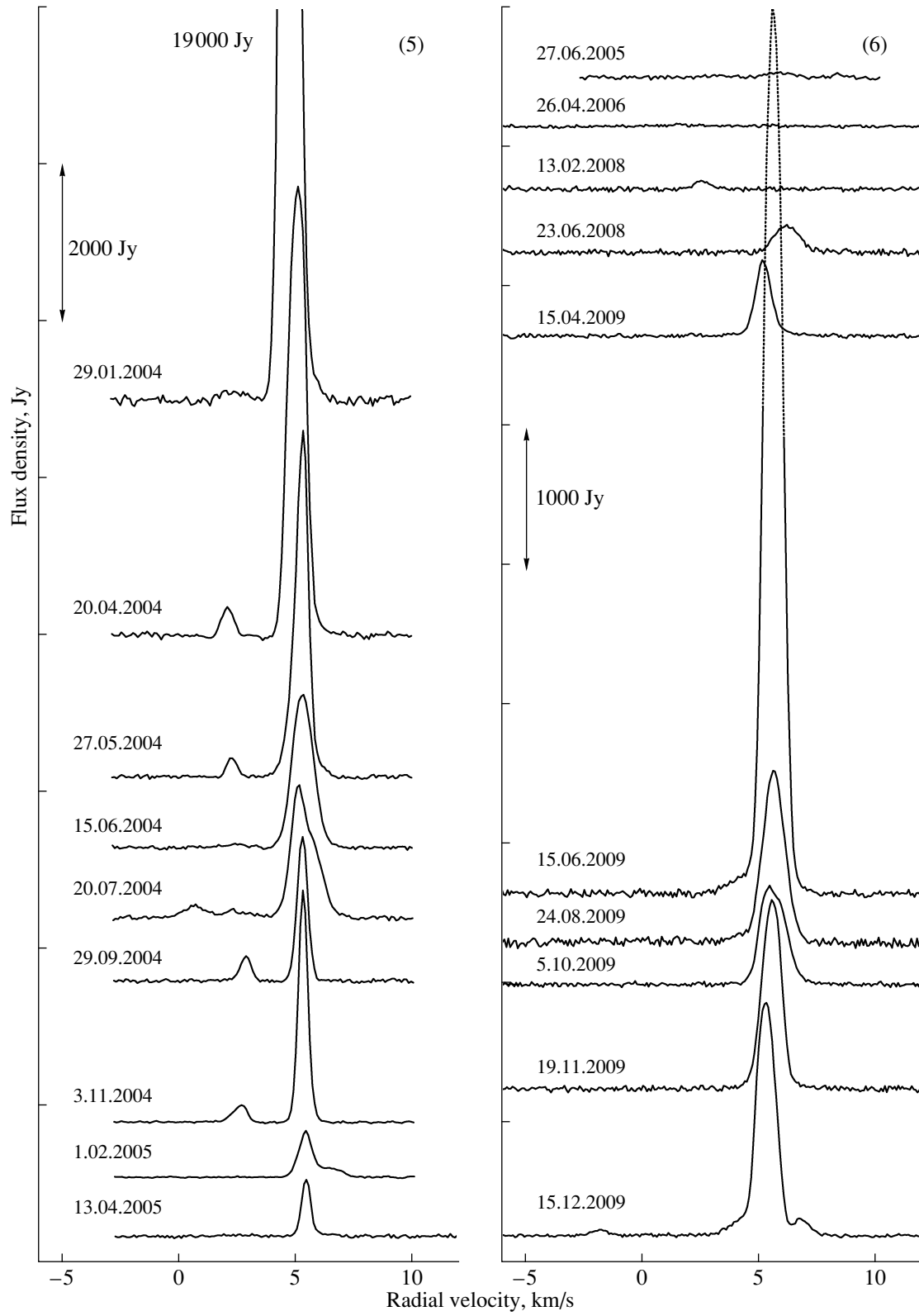


Fig. 3. H_2O maser spectra for IRAS 16293-2422 in 2004-2009.

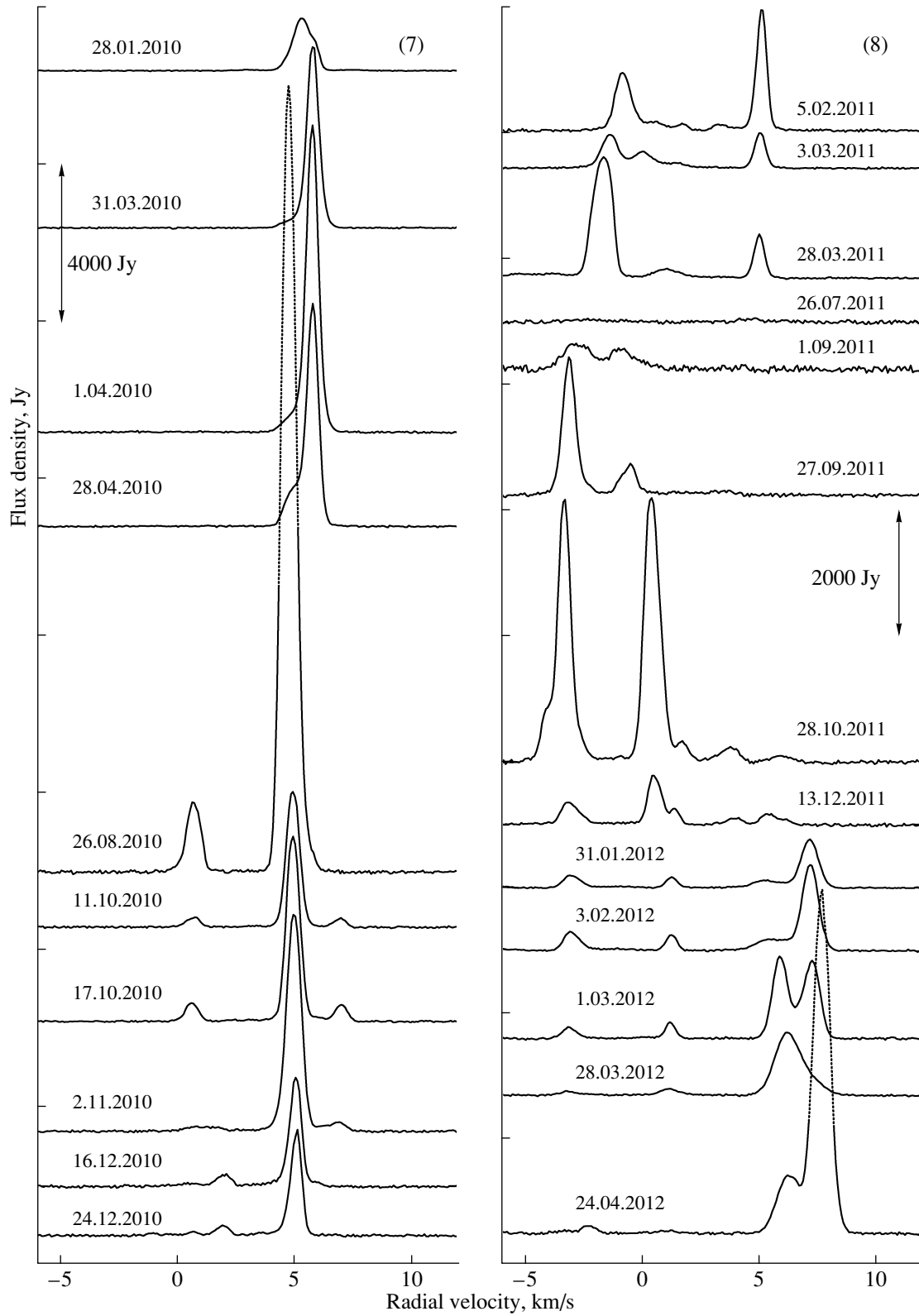


Fig. 4. H₂O maser spectra for IRAS 16293–2422 in 2010–2012.

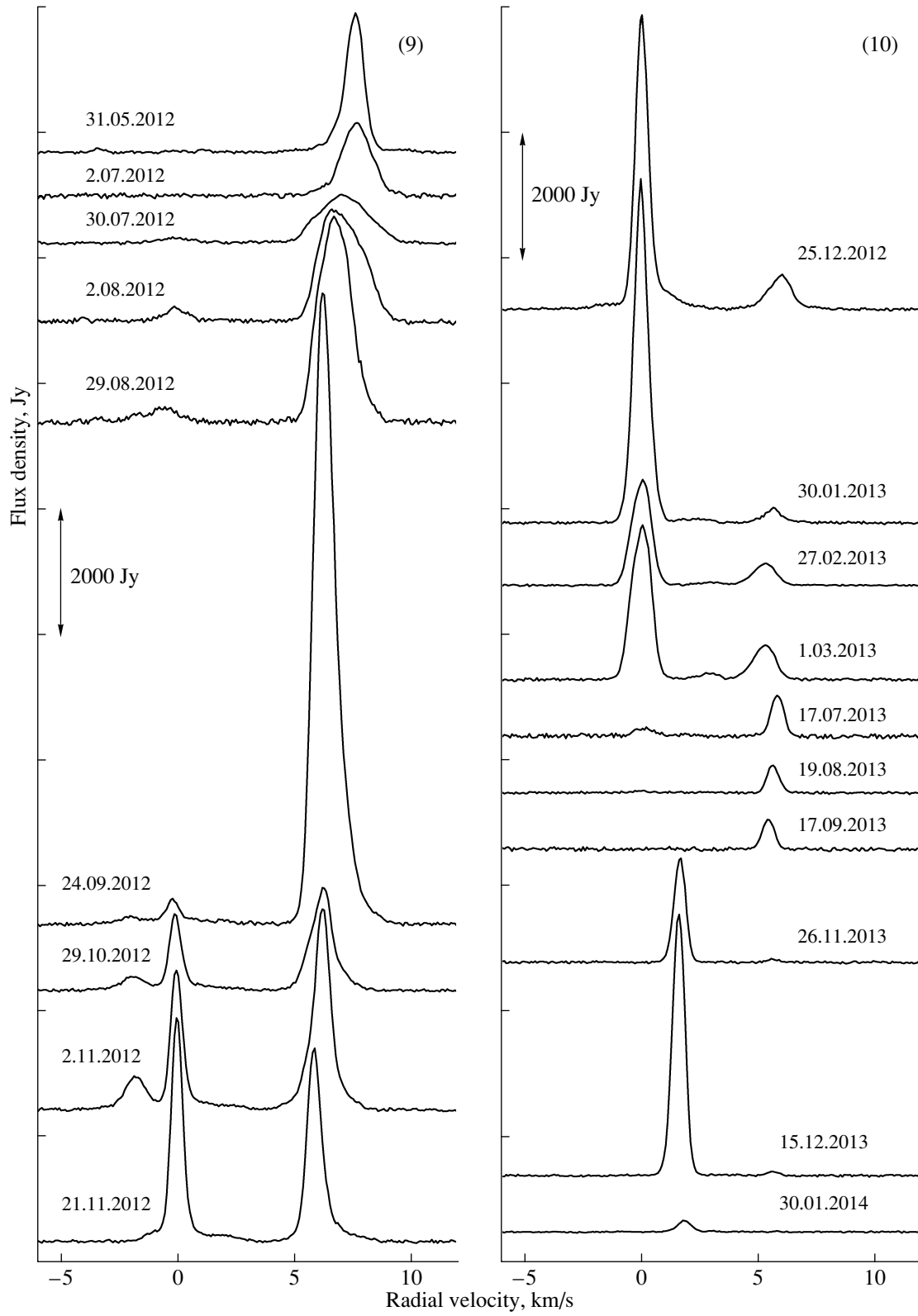


Fig. 5. H₂O maser spectra for IRAS 16293–2422 in 2012–2014.

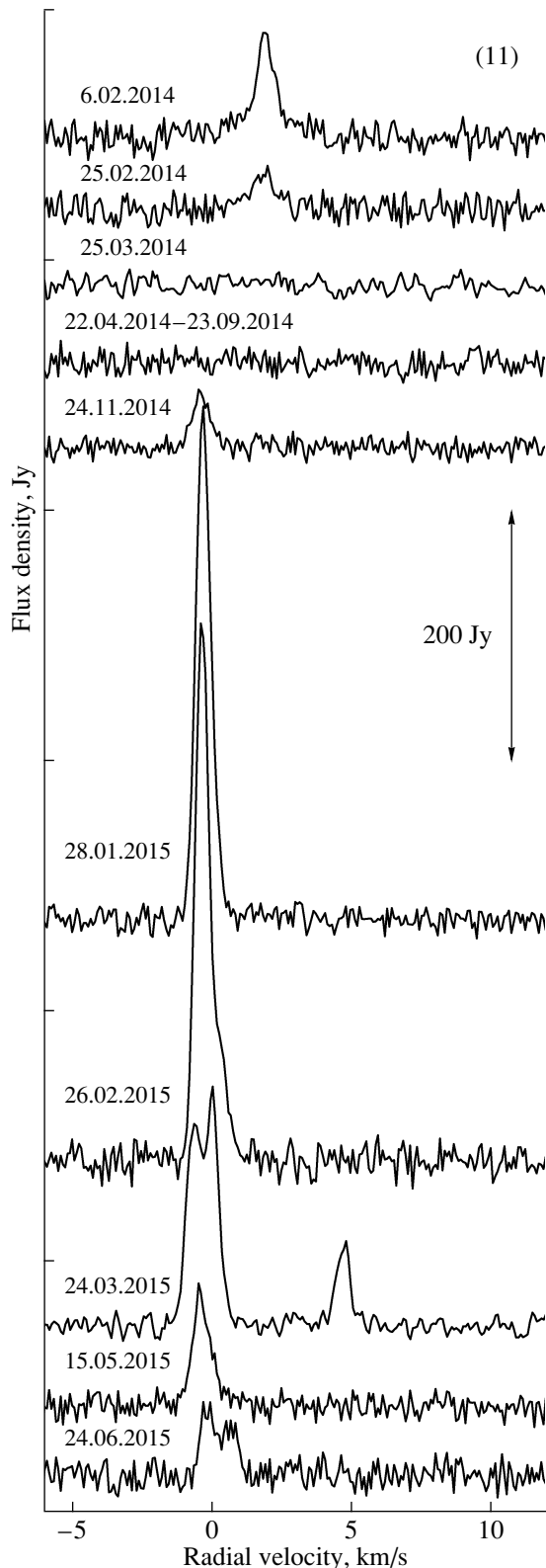


Fig. 6. H₂O maser spectra for IRAS 16293–2422 in 2014–2015.

other very strongly in the intensity of the flares of individual features and groups of features, and also

in the structure of the spectra. The flares were often very short. Flares were frequently followed by short periods of very low maser activity. The longest minima with very low levels of maser emission occurred in mid-2000, 2005–2006, and 2014. Thus, we conclude that the activity of the water-vapor maser in IRAS 16293–2422 has a cyclic character.

The main H₂O maser emission was observed in two velocity ranges: 4.3–7.5 km/s and –3–2.5 km/s. The first represents a red shift relative to the velocity of the molecular cloud and the second a blue shift. In the first range, we observed emission from a fairly large number of features. The emission that was strongest and appeared most often was near a radial velocity of 5 km/s. The main emission in the second velocity range above was near radial velocities of –3, 0, and ~2.4 km/s. The region emitting near zero radial velocity probably has a complex structure.

In addition to studying the evolution of groups of features with similar radial velocities during periods of high activity (flares), it is of interest to study the flares of individual features. We analyzed the line shapes for such features at the epochs of their maximum activity. Important parameters here are the symmetry or asymmetry of the line and the shape of the line's wings and their evolution with the development of the flare. This analysis revealed a larger number of components than in the case of simple Gaussian fitting, and enabled the detection of possible turbulent motions of the matter.

Our analysis shows that the line widths of individual features lie in a narrow radial-velocity range: 0.6–0.8 km/s. Both symmetric and asymmetric line shapes are observed. Symmetric lines are reproduced well by Gaussian fits. However, in some cases, one (left or right) or both wings lay above the Gaussian fit.

3.1. Flares at Velocities of 4.3–7.5 km/s

Configuration 1 (Fig. 7) has a simple structure. The main feature is at a velocity of about 7.4 km/s and had a maximum emission during a short-term flare of 720 Jy. We did not detect any drift in excess of 0.15 km/s.

During the strongest H₂O maser flare in 2003–2004 ($F_{\max} = 16\,700$ Jy), the shock successively excited three main features with distinct but similar radial velocities (from 4.6 to 5.4 km/s). This is clearly seen in Figs. 1 and 2 (panels 2 and 3), Fig. 7 (structures 2 and 3), and Fig. 9. Features were excited by the shock not simultaneously, but with time delays, indicating that the features are spatially separated. According to Imai et al. [20] who observed this emission during the same time interval, the emission exhibited a drift in space as well as in velocity. However,

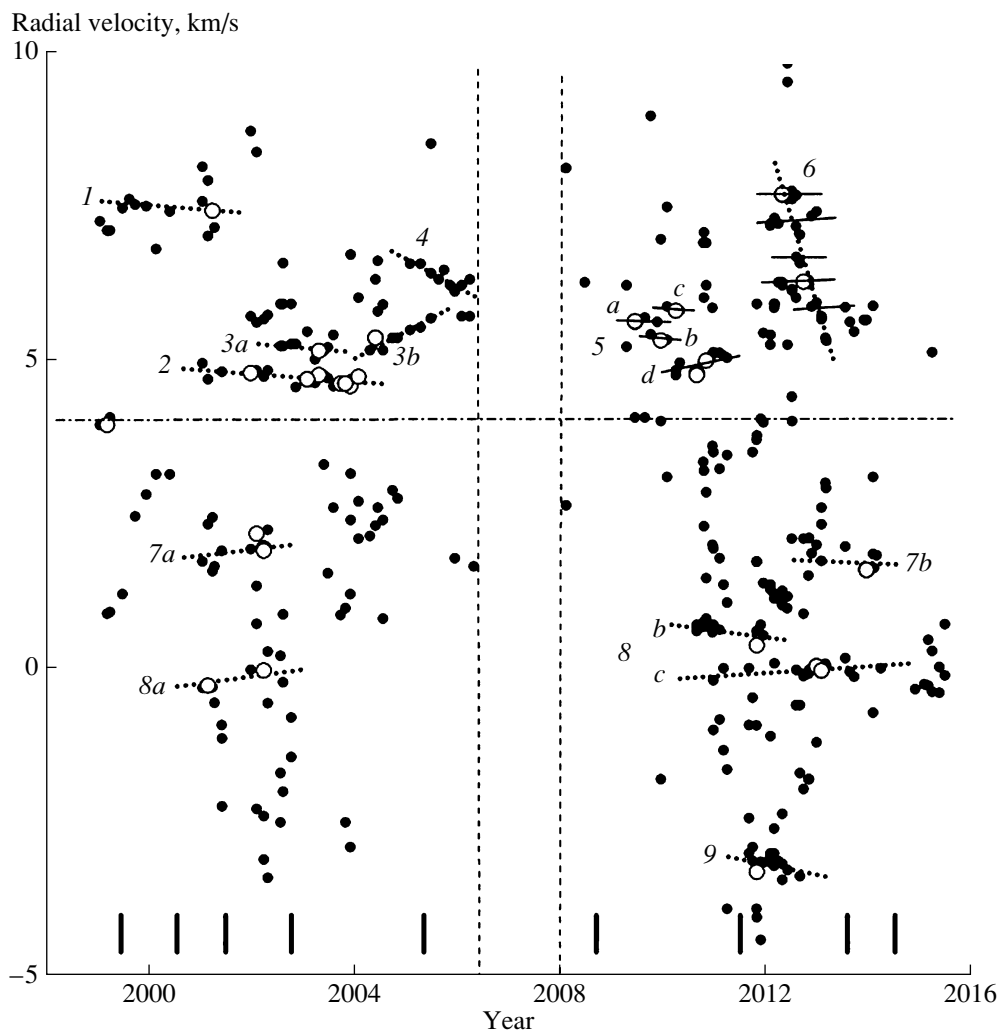


Fig. 7. Radial-velocity variations of the main H₂O maser emission features. Features observed during epochs of high activity (strong flares) are plotted as open circles. The vertical lines mark epochs of minimum activity. The horizontal dash–dot line shows the velocity of the CO molecular cloud (4 km/s). The positions of the flux maxima for features with similar radial velocities (the drift of these maxima) were approximated by the numbered straight dashed lines. There were no observations in the time interval between the two vertical dashed lines for technical reasons.

we believe that we are dealing with two effects here. The first is real proper motions of the features, and the second one is the sequential excitation of emission from spatially separated features with similar radial velocities during the flare.

Figure 9 shows the central parts of H₂O emission line profiles. We normalized the profiles for convenience in analyzing their evolution. The observing epochs are indicated. The normalized profiles for the first three epochs agree well in both the line shape and velocity (4.6 km/s). We fitted each of these with a Gaussian curve, which approximated the profile well. For all three epochs, we observed a deviation from the Gaussian curve in the right wings, due to the presence of a weaker feature in the line wing, at a

velocity of 5.4 km/s. We conclude from the character of the profile's evolution that at least three emission features are present, at 4.6, 5.0, and 5.4 km/s. The times when the velocity of the emission maximum changed coincide with those determined by Imai et al. [20].

A similar morphology of the maser was also noted by Alves et al. [17] at a different epoch (2007). According to [17], the shape of the spectrum in 2007 was not Gaussian: there were at least three features (at 5.7, 7.4, and 9.2 km/s) that formed a linear configuration. The features were excited by a front of compressed gas in the molecular outflow activated by the protostar.

The evolution of the flare in 2009–2010 was very

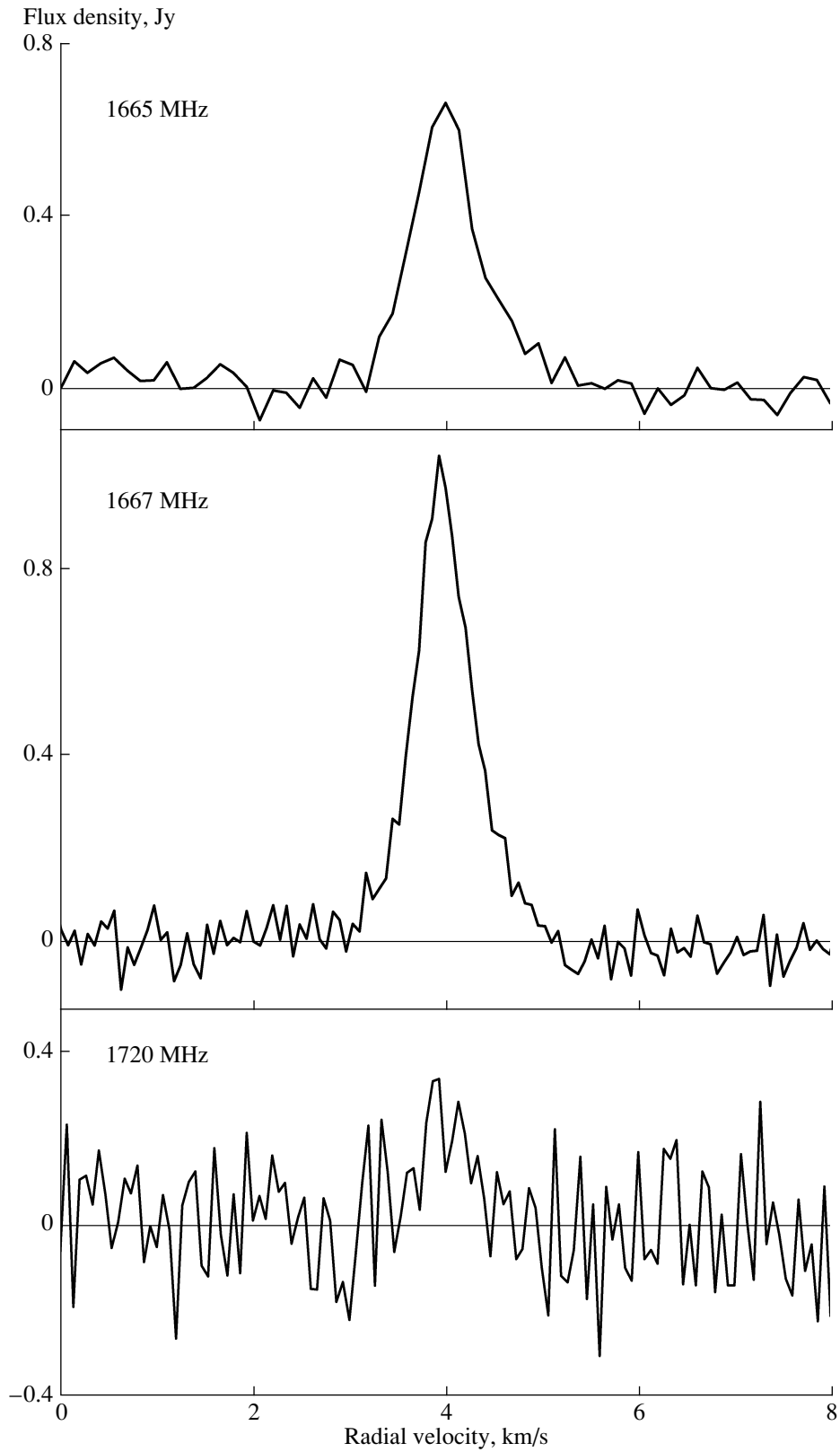


Fig. 8. Emission profiles in the 18-cm hydroxyl lines in the direction of IRAS 16293–2422 (see the text).

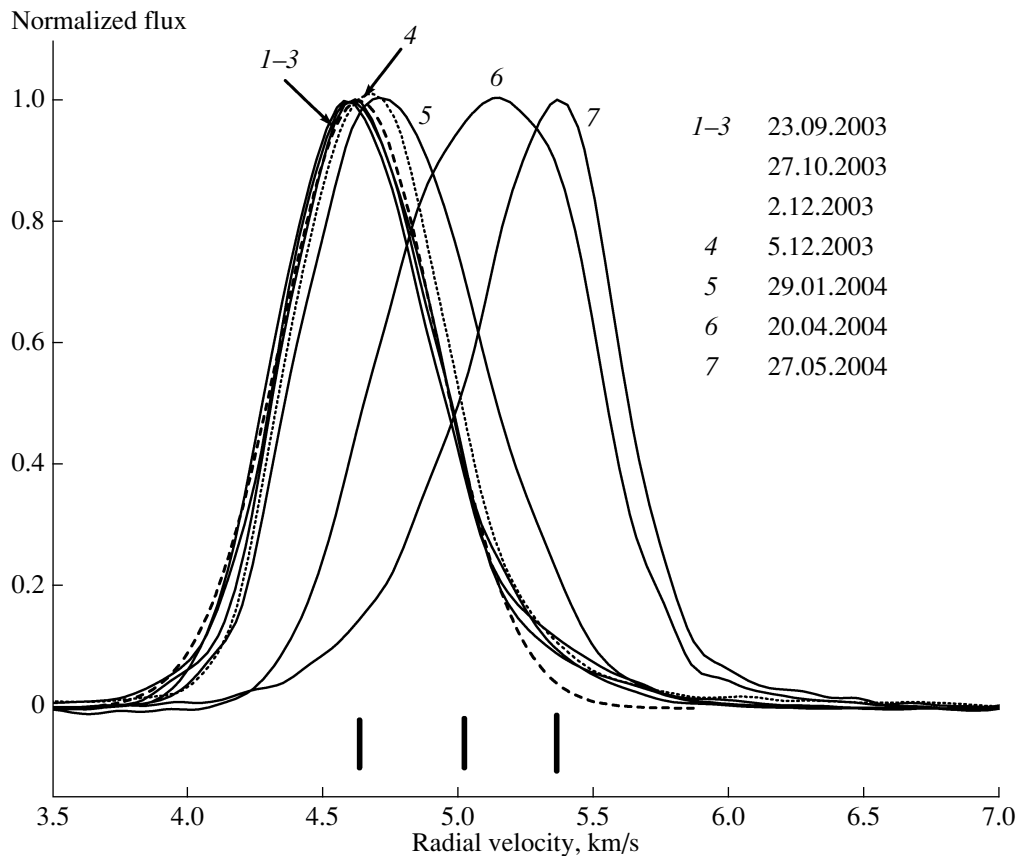


Fig. 9. Normalized H₂O emission profiles during the strongest flare of IRAS 16293–2422 in 2003–2004. The dotted curve is the profile at the beginning of the strong changes of its structure. The observing epoch is indicated for each line profile. The dashed curve is a Gaussian fit to the profile at the emission maximum (45 000 Jy in October 2003). The vertical bars in the lower part of the figure mark the radial velocities of the main features of the flare.

complex. A sequence of flares of the four main features was observed (Figs. 4 and 7). This structure is marked 5 in Fig. 7, with the four components labeled as *a*, *b*, *c*, and *d*. We find no structure ordered in velocity. The spectrum evolution can best be explained in a model with an arc (e.g., [22]), or simply a cluster, of maser features.

The strong flare of 2012–2013 also had a very complex evolution. The strongest emission, with a flux of about 10 000 Jy, was at $V_{\text{LSR}} = 6.24$ km/s. The flare was also accompanied by a strong drift of the emission maximum at a rate of about 3 km/s per year. This drift was due to features with velocities from 7.5 to 5.3 km/s being consecutively excited (see Figs. 4 and 5, panels 8–10, and the structure 6 in Fig. 7). These features may form a spatial structure with a radial-velocity gradient, for instance, in the form of a chain. Such formations are usually called organized structures.

We identified five features based on the character of the line-profile evolution, marked in Fig. 7 with straight lines. The delays between the flux maxima of these features were from 0.16 to 0.35 years. The

maser could be pumped with a shock propagating from the star. Ristorcelli et al. [23] demonstrated the presence of a shock in IRAS 20126 using data on the submillimeter water emission.

The modeling of these data carried out by Kaufman and Neufeld [24] yielded evidence for a C shock with a velocity of about 12–15 km/s in the neighborhood of IRAS 20126. For a velocity of 15 km/s, the delays detected in the observations correspond to distances between the features (perpendicular to the shock front) from 0.5 to 1.1 AU, and to a total length for the chain of ~ 2 AU. This is in a good agreement with results for other sources, such as W75N [22, 25].

3.2. Emission at Velocities -1.5 – 2.1 km/s

Figure 10 presents profiles of the H₂O emission lines at velocities near 0 km/s during epochs of flares (the structure 8 in Fig. 7). Since the flux range during the flare maxima differed only slightly, we plotted all the profiles using the same scale (Fig. 10a). The weaker flare of 2015 is shown separately in Fig. 10b,

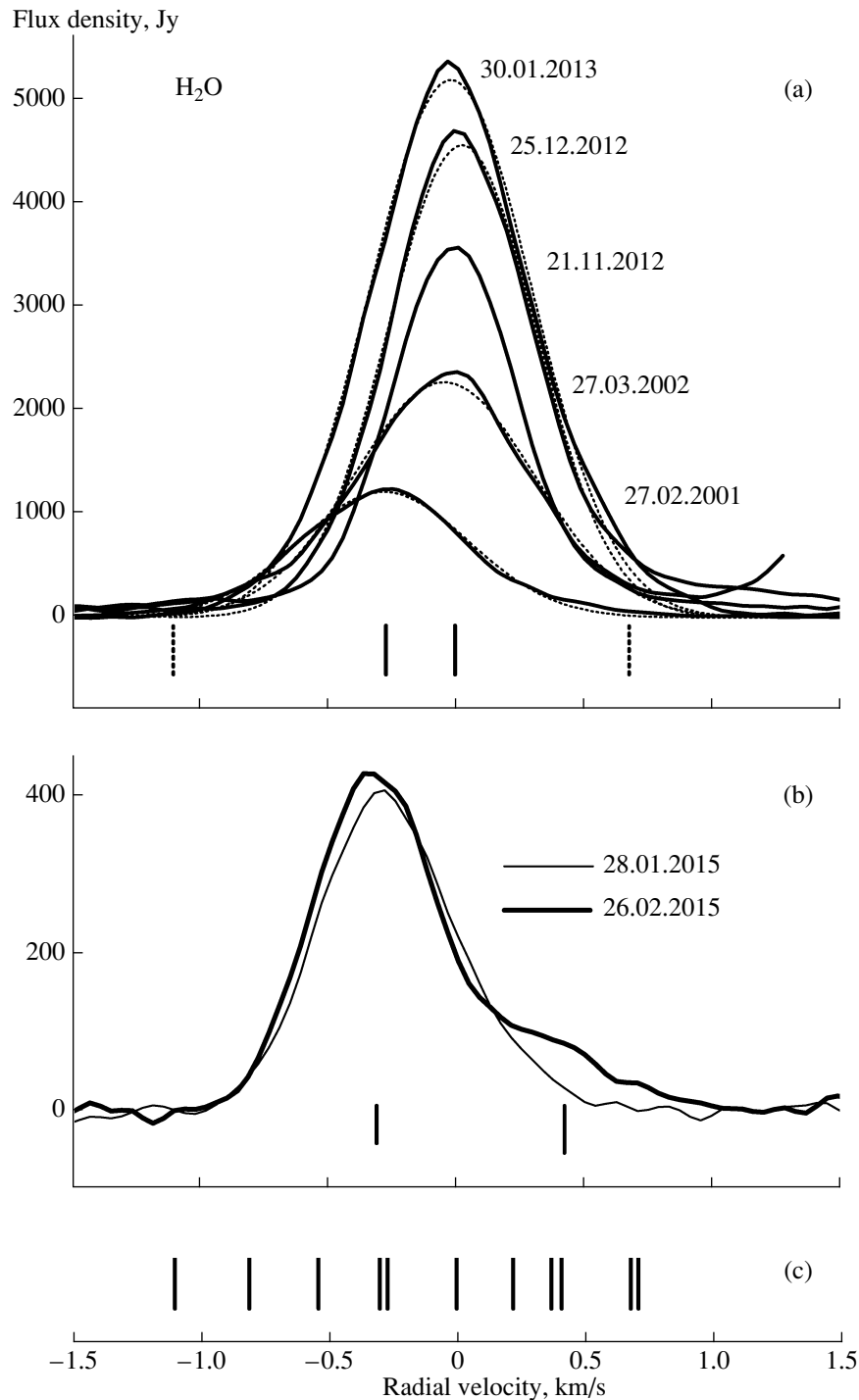


Fig. 10. (a) Line profiles of H₂O emission features at velocities near 0 km/s during epochs of maximum emission. The observing epochs are indicated to the right of the maxima. The dotted curves are Gaussian fits. (b) H₂O line profiles during the flare in 2015. The vertical bars mark features identified for every flare. (c) Positions of all emission features with fluxes exceeding 800 Jy that were observed in the course of our monitoring since 1999.

with fitted Gaussian curves. The line profiles are not quite symmetric, with slight deviations from a Gaussian shape. The reason for this could be that the observed maser condensations are not homogeneous.

It is surprising that, between 2002 and 2013, emission appeared infrequently, but always at a velocity close to 0 km/s.

The flare in 2015 occurred at the same velocity

as in 2001 (-0.3 km/s). All this may indicate that the maser condensations at these velocities are fairly stable formations. The solid vertical bars in Fig. 10 mark the main flare components, and the dashed bars components with fluxes below 100 Jy. In Fig. 10c, we have marked the positions of all emission features with fluxes higher than 800 Jy observed in the course of our monitoring since 1999. Many of these flares had short durations, comparable to the time intervals between our observations.

Finally, let us consider the emission near 2 km/s. These emission features form structure 7 in Fig. 7. Mainly, weak emission was observed at these velocities. We can identify two strong, short-lived flares in 2002 and 2014, at velocities of 1.9 and 1.7 km/s, respectively. These flares were accompanied by short-lived features appearing at 1.6–2.1 km/s. We found no regular pattern in the appearance of the emission at these velocities, indicating that this configuration of the H₂O maser has a complex structure, and is most probably associated with a cluster of individual maser features.

3.3. Characteristic Properties of the H₂O Maser in IRAS 16293–2422

We found a number of characteristic properties of the H₂O maser emission in IRAS 16293–2422, compared to many similar sources associated with cool IR sources (see, e.g., [26]).

- The main difference is the large number of very strong flares.
- During strong flares, emission was observed in a narrow range of radial velocities (from 4.5 to 6 km/s). As a rule, there was no emission from other features, even weak ones.
- Very short flares were usually associated with individual features and appeared at random times (Fig. 7).
- During 1987–1992, the highest maser activity was at radial velocities of 6–8 km/s [14, 15, 27, 28]. Our present study indicates that the most prominent activity moved to 4.5–5.5 km/s during 2001–2004 and 2009–2010. In 2012, the activity again moved, to the 5.5–7.5 km/s. In addition, fairly strong emission was observed near zero velocity, with weaker emission in a wide radial-velocity range.

Beginning with late 2012, the emission at $V_{\text{LSR}} = 5$ km/s decreased sharply, but emission appeared near zero velocity, reaching a flux of 5500 Jy in January 2013. Towards the end of 2013, a strong, short-term flare (4200 Jy) occurred at 1.6 km/s. Finally, a weaker flare occurred in 2015, again near the zero velocity.

Thus, there exist preferred radial-velocity ranges (-0.3 – 0.4 , 1.6–2.1, and 4.5–5.5 km/s) where powerful maser emission with a flare nature was observed.

3.4. Hydroxyl Emission

The hydroxyl emission from IRAS 16293–2422 was unpolarized at all our observing epochs. The flux in the 1665, 1667, and 1720 MHz lines were in the proportion 4 : 2.7 : 1. These proportions differ slightly from the classic values for thermal emission. The radial velocity of the emission maximum was at about 4 km/s, coincident with the velocity of the CO cloud, and the line widths were ~ 0.7 km/s. This hydroxyl emission is most probably thermal. In this case, a line width of 0.7 km/s corresponds to a temperature for the region of hydroxyl emission of ~ 30 K, close to the usual temperatures of warm clouds where cool IR sources are situated (40 K).

In addition to the main component, there is a weak component in the right wings of the main lines. This component is somewhat stronger in the 1665 MHz line than in the 1667 MHz line, and its radial velocity is 4.6–4.8 km/s. This line shape may reflect non-uniform structure of the cloud, which may contain two condensations of matter.

4. CONCLUSIONS

We have presented the results of our monitoring of the very young cool IR source IRAS 16293–2422. Interpreting our data, we also used numerous observations (monitoring and high-angular-resolution) of this source from other studies. Below we list the main results of this study.

- The H₂O maser emission exhibited a sequence of strong flares, sometimes with fluxes reaching tens of thousands of Jansky, with an absence of persistent emission.
- Individual H₂O maser features can form organized structures in the form of chains ~ 2 AU long, along which regular velocity variations are observed.

- The proper motions of H₂O maser features at 4.3–5.3 km/s (2003–2004) are probably lower than is suggested by observations with high angular resolution. The reason for this may be a complex structure with a cluster of maser features (with similar radial velocities and separated by small distances) that are successively excited by a shock formed in the molecular outflow during flares of activity. Thus, different features are observed one after another at different epochs.
- The maser condensations responsible for the emission at velocities between –1.5 and 1.6 km/s are probably stable structures.
- The emission in the 1665, 1667, and 1720 MHz lines of the hydroxyl molecule is unpolarized and thermal. The observed line width, ~0.7 km/s, corresponds to a temperature of about 30 K for the formation region of the thermal OH radiation.

ACKNOWLEDGMENTS

The authors thank staff of the Pushchino (Russia) and Meudon (France) Radio Astronomy Observatories for their invaluable assistance during the observations.

This study was supported by the Russian Foundation for Basic Research (project code 15-02-07676).

REFERENCES

1. J. Knude and E. Hog, *Astron. Astrophys.* **338**, 897 (1998).
2. J. C. Correia, M. Griffin, and P. Saraceno, *Astron. Astrophys.* **418**, 607 (2004).
3. L. G. Mundy, B. A. Wilking, and S. T. Myers, *Astrophys. J.* **311**, L79 (1986).
4. L. G. Mundy, A. Wootten, B. A. Wilking, G. A. Blake, and F. I. Sargent, *Astrophys. J.* **385**, 306 (1992).
5. L. W. Looney, L. G. Mundy, and W. J. Welch, *Astrophys. J.* **529**, 477 (2000).
6. C. J. Chandler, C. L. Brogan, Y. L. Shirley, and L. Loinard, *Astrophys. J.* **632**, 371 (2005).
7. C. D. Lada and B. A. Wilking, *Astrophys. J.* **238**, 620 (1980).
8. J. G. A. Wouterloot, K. Fiegle, J. Brand, and G. Winnewisser, *Astron. Astrophys.* **301**, 236 (1995).
9. B. A. Wilking and C. J. Lada, *Astrophys. J.* **274**, 698 (1983).
10. C. K. Walker, C. J. Lada, E. T. Young, and M. Margulis, *Astrophys. J.* **332**, 335 (1988).
11. S. C. C. Yeh, N. Hirano, T. L. Bourke, P. T. P. Ho, C.-F. Lee, N. Ohashi, and S. Takakuwa, *Astrophys. J.* **675**, 454 (2008).
12. R. Rao, J. M. Girart, D. P. Marrone, S. Lai, and S. Schnee, *Astrophys. J.* **707**, 921 (2009).
13. G. Narayanan, C. K. Walker, and H. D. Buckley, *Astrophys. J.* **496**, 292 (1998).
14. B. A. Wilking and M. J. Claussen, *Astrophys. J.* **320**, L133 (1987).
15. S. Terebey, S. N. Vogel, and P. C. Myers, *Astrophys. J.* **390**, 181 (1992).
16. C. J. Chandler, C. L. Brogan, Y. L. Shirley, and L. Loinard, *Astrophys. J.* **632**, 371 (2005).
17. F. O. Alves, W. H. T. Vlemmings, J. M. Girart, and J. M. Torrelles, *Astron. Astrophys.* **542**, A14 (2012).
18. R. S. Furuya, Y. Kitamura, A. Wootten, M. J. Claussen, and R. Kawabe, *Astrophys. J. Suppl.* **144**, 71 (2003).
19. H. Imai, T. Iwata, and M. Miyoshi, *Publ. Astron. Soc. Jpn.* **51**, 473 (1999).
20. H. Imai, K. Nakashima, T. Bushimata, Y. K. Choi, T. Hirota, M. Honma, K. Horiai, N. Inomata, K. Iwadate, T. Jike, O. Kameya, R. Kamohara, Y. Kan-Ya, N. Kawaguchi, M. Kijima, et al., *Publ. Astron. Soc. Jpn.* **59**, 1107 (2007).
21. W. G. L. Pöppel and E. Scalise, Jr., *Rev. Mex. Astron. Astrofíz.* **17**, 121 (1989).
22. E. E. Lekht, V. I. Slysh, and V. V. Krasnov, *Astron. Rep.* **51**, 967 (2007).
23. I. Ristorcelli, E. Falgarone, F. Schöier, S. Cabrit, M. Gerin, Ph. Baron, U. Frisk, J. Harju, A. Hjalmarsson, A. Klotz, B. Larsson, R. Liseau, and L. Pagani, *IAU Symp.* **235**, 227 (2005).
24. M. J. Kaufman and D. A. Neufeld, *Astrophys. J.* **456**, 250 (1996).
25. J. M. Torrelles, J. F. Gómez, L. F. Rodríguez, P. T. P. Ho, S. Curiel, and R. Vázquez, *Astrophys. J.* **489**, 744 (1997).
26. P. Colom, E. E. Lekht, M. I. Pashchenko, G. M. Rudnitskii, and A. M. Tolmachev, *Astron. Lett.* **41**, 425 (2015).
27. M. Felli, F. Palagi, and G. Tofani, *Astron. Astrophys.* **255**, 293 (1992).
28. M. J. Claussen, B. A. Wilking, P. J. Benson, A. Wootten, P. C. Myers, and S. Terebey, *Astrophys. J. Suppl.* **106**, 111 (1996).

Translated by N. Samus'